Topological swarmalators

Jun-Bo Gou (勾俊博),[1,2] Marc Timme,[3,4] Xiaozhu Zhang (张潇竹),[1,2,3,*] and Gang Yan (严钢)[1,2,†]

[1]*MOE Key Laboratory of Advanced Micro-Structured Materials, and School of Physical Science and Engineering, Tongji University, Shanghai, People's Republic of China*

[2]*National Key Laboratory of Autonomous Intelligent Unmanned Systems, MOE Frontiers Science Center for Intelligent Autonomous Systems, and Shanghai Research Institute of Intelligence Science and Technology, Tongji University, Shanghai, People's Republic of China*

[3]*Chair for Network Dynamics, Center for Advancing Electronics Dresden (cfaed), Institute for Theoretical Physics, and Center for Synergy of Systems, TUD Dresden University of Technology, 01062 Dresden, Germany*

[4]*Lakeside Labs, Lakeside B04b, 9020 Klagenfurt, Austria*

(Received 9 July 2025; accepted 16 December 2025; published 20 January 2026)

Swarmalators constitute a paradigmatic model for understanding the collective dynamics of coupled moving agents, integrating both internal and spatial degrees of freedom. Empirical evidence from systems such as bird flocks and living matter highlights the relevance of topological, metric-free coupling, but their impact on swarmalator dynamics remains largely unknown to date. Here, we present and analyze a topological swarmalator model in which the units interact topologically, on Delaunay networks. We find intriguing self-organized collective dynamics, including patterns with local vortices and unprecedented spatiotemporal patterns absent in metric-based models. Identifying three order parameters to quantify synchrony, spatial order, and vortex formation, we map the phase diagram that classifies these diverse patterns. Notably, we uncover a first-order transition even if the phases of all units are frozen, a dynamics inverted relative to the classical Kuramoto model. These insights not only advance our theoretical understanding of locally coupled systems of moving agents, but also offer key guidelines for their control.

DOI: 10.1103/kghb-vpst

I. INTRODUCTION

The collective dynamics of systems of units with simple local interactions often exhibits striking large-scale patterns [1–7]. Paradigmatic models by Kuramoto [8] and Vicsek *et al.* [9] have inspired extensive research on their nonlinear dynamics and statistical physics, particularly to understand their fundamental temporal and spatial ordering phenomena—synchronization and flocking. More recently, systems combining spatial and phase dynamics [10–13]—termed "swarmalators" [12]—have attracted attention for their rich self-organized behavior [14–17] and potential applications in decentralized robotics [18–21]. Interesting patterns have since been found in swarmalator systems within one-dimensional (1D) space [22–28], with time-varying or delayed couplings [29–33], and heterogeneous parameters or higher-dimensional dynamics [34–38].

However, most swarmalator studies assumed all-to-all or metric-based interactions, despite empirical evidence that real systems—from bird flocks [39] to living matter [40–45]—often rely on topological interactions. These interactions maintain cohesion more robustly and lead to critical properties different from known universality classes [46], yet their role in swarmalator dynamics remains largely unexplored.

In this article, we introduce a topological swarmalator model where interactions are defined via nearest neighbors in a Delaunay triangulation. Coupling via such Delaunay network coupling yields collective behaviors and qualitatively different patterns not seen in metric-based models [46,47], especially the emergence of local vortices. We introduce three order parameters to map the whole phase diagram by systematically classifying the complex behaviors into seven distinct spatiotemporal patterns. Notably, even when the units' phases are frozen—a state inverted relative to the classical Kuramoto model—the system undergoes a first-order transition.

II. MODEL

Let us consider the collective dynamics of systems of N swarmalator governed by [12]

$$\dot{\boldsymbol{x}}_i = \boldsymbol{v}_i + \sum_{\langle ij \rangle} \frac{\boldsymbol{x}_{ji}}{\|\boldsymbol{x}_{ji}\|}(A + J\cos(\theta_j - \theta_i)) - B\frac{\boldsymbol{x}_{ji}}{\|\boldsymbol{x}_{ji}\|^2},$$

$$\dot{\theta}_i = \omega_i + K\sum_{\langle ij \rangle} \frac{\sin(\theta_j - \theta_i)}{\|\boldsymbol{x}_{ji}\|}. \tag{1}$$

Here, $\boldsymbol{x}_i(t) = (x_i(t), y_i(t))^{\mathsf{T}} \in \mathbb{R}^2$ is the position of the ith unit at time t, and the parameters $\boldsymbol{v}_i$, $\omega_i \in \mathbb{R}$ are its self-propulsion

*Contact author: xiaozhu_zhang@tongji.edu.cn
†Contact author: gyan@tongji.edu.cn

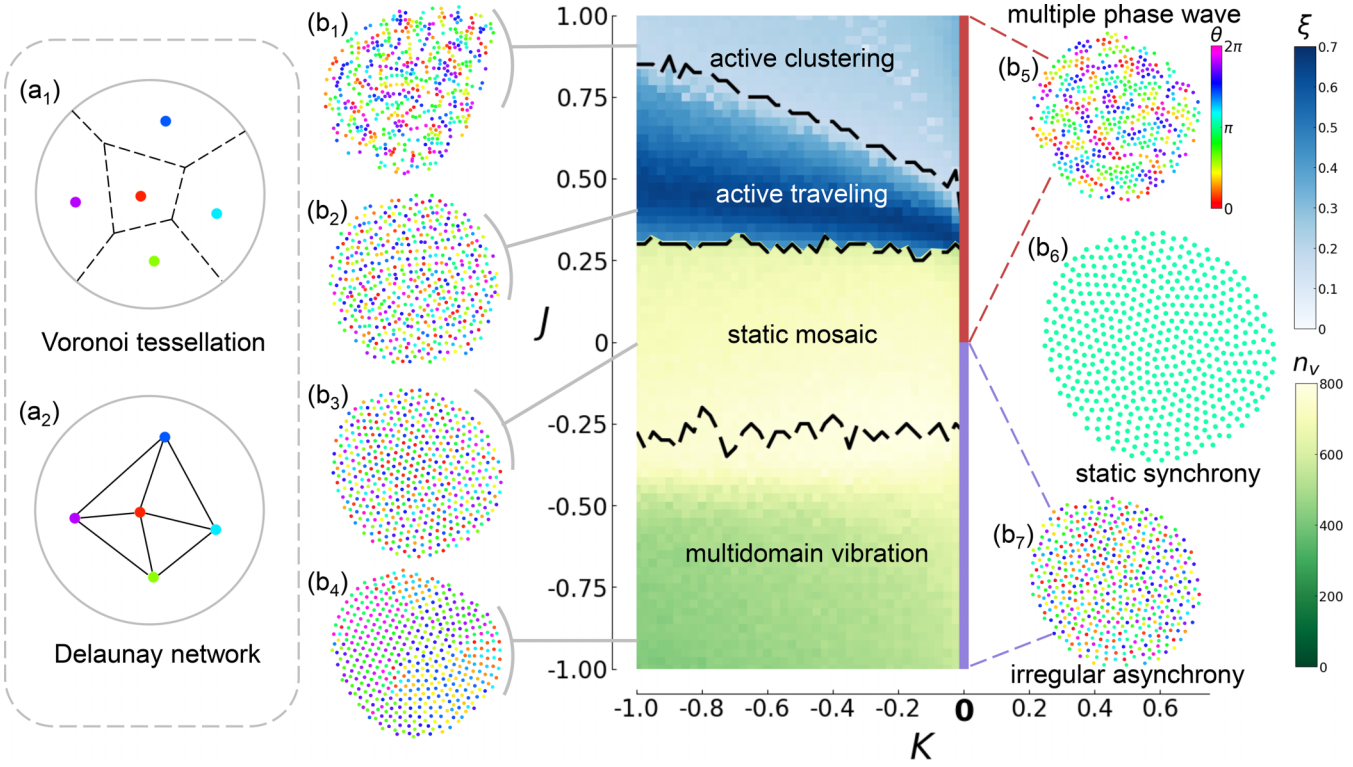

FIG. 1. Phase diagram of two-dimensional (2D) topological swarmalators. (a) Illustration of (a_1) the Voronoi tessellation constructed from the current positions of all units, with (a_2) the associated Delaunay network defining each unit's nearest neighbors. (b) Seven collective patterns (b_1)–(b_7) discovered in the 2D topological swarmalators, composed of 500 units evolving according to Eq. (1) in the (K, J) plane (see Video in the Supplemental Material [48] for dynamic evolution). The boundaries are denoted by the vertical line at $K = 0$ and the three black dashed lines that indicate abrupt changes in the correlation length ξ and the total vortex number n_v. As initial states, swarmalators are randomly and uniformly distributed within a square, with their phases drawn from a uniform distribution over $[0, 2\pi)$.

velocity and natural frequency, respectively. The position difference vector $\boldsymbol{x}_{ji} = \boldsymbol{x}_j - \boldsymbol{x}_i$ for two units i and j yields their Euclidean distance $\|\boldsymbol{x}_{ji}\| := \sqrt{(x_j - x_i)^2 + (y_j - y_i)^2}$. The key distinction from metric-based models lies in the topological definition of interactions $\langle ij \rangle$ between swarmalators i and j, where neighbors are determined by the Delaunay network constructed from the instantaneous positions of all units [Figs. 1(a_1) and 1(a_2)]. We fix $A = B = 1$ by rescaling time and space. To understand the impact of the interplay between position and phase, we focus on homogeneous systems with $\omega_i = \boldsymbol{v}_i = 0$ for all units such that state heterogeneities emerge from the (random) initial conditions. The system is then governed by only two parameters: J, controlling how phase differences affect spatial motion $\dot{\boldsymbol{x}}_i$, and K, controlling how strongly topological proximity influences phase dynamics $\dot{\theta}_i$. Generalizations, e.g., to distributed frequencies, exhibit similar collective dynamics as well as additional states such as partially phase-locked states (see the Supplemental Material [48]).

III. PHASE DIAGRAM

The topological interactions between swarmalators yield a variety of collective dynamics [see Figs. 1(b_1)–1(b_7) and the Video in the Supplemental Material [48]], including emergent patterns exhibiting local vortices, several of which have not been observed in fully connected or metric-based swarmalators.

To distinguish these diverse patterns, we quantify spatial order of phases, temporal order (synchrony), and vortex formation by three order parameters. First, we quantify the exponential decay of the radial correlation function

$$\langle \theta(r)\theta(0) \rangle \propto \exp(-r/\xi) \tag{2}$$

by its correlation length ξ. Here, $r = \|\boldsymbol{x}_{ij}\|$ denotes the spatial distance between pairs of units and $\langle \cdot \rangle$ denotes the averaging over all pairs separated by distance r. Second, we quantify synchrony among units by the degree of phase coherence as [49]

$$R = \sum_{\langle ij \rangle} \cos(\theta_j - \theta_i). \tag{3}$$

Third, we count the total number of vortices in a pattern as

$$n_v = \sum_{\text{triangles}} \left| \oint \frac{\nabla\theta \cdot d\boldsymbol{r}}{2\pi} \right|, \tag{4}$$

which evaluates whether each triangle consisting of three neighboring units forms a vortex or antivortex (see Fig. 2 for an illustration).

For $K > 0$, all units become synchronized, sharing the same phase and distributing uniformly in space—an arrangement we refer to as *static synchrony* [Fig. 1(b_6)].

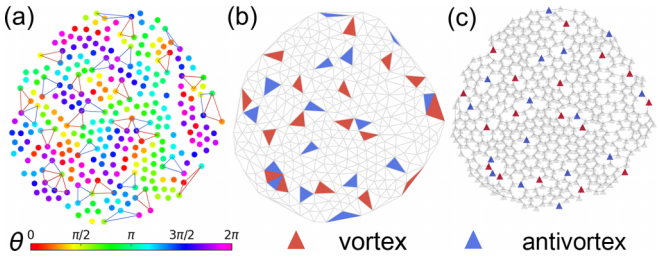

FIG. 2. Emerging vortices in topological swarmalators. (a) After a transient process, several unprecedented steady-state patterns emerge due to topological interactions, with "multiple phase waves" shown here. (b) The nearest-neighbor interaction topology among swarmalators, determined via Delaunay triangulation. A triangle is identified as a vortex (red) if the swarmalator phases decrease in a clockwise direction, and as an antivortex (blue) if the phases follow a counterclockwise arrangement. (c) The dual graph of panel (b), where nodes correspond to the triangles in panel (b).

In contrast, for $K < 0$, neighboring units tend to adopt phases differing by π, forming antiphase relationships. This antagonistic phase coupling gives rise to diverse collective patterns, depending on the sign and strength of J. Notably, vortices can spontaneously emerge, where groups of units locally self-organize into coherent rotational motion (Fig. 2). Such collective dynamics resembles experimental observations in different active matter systems [40–43,45], yet is not captured by the original swarmalator model [12]. We find that qualitative changes of the correlation length ξ and the number n_v of vortices delineate the boundaries between four distinct motion patterns (see Fig. 1 as well as Figs. S1—S2 and Sec. I in the Supplemental Material [48]). For J sufficiently close to zero, phase differences exert weak influence on the collective motion, resulting in a disordered yet evenly distributed spatial configuration in which swarmalators tend to have maximally opposite phases from their neighbors [*static mosaic*, Fig. 1(b_3)].

For strongly negative J, the swarmalators vibrate around their constant average positions within separate domains. Within each domain, neighbors maintain fixed phase differences, but the phase orientations vary across domains due to the interplay between spatial attraction and the preference for antiphase alignment [*multidomain vibration*, Fig. 1(b_4)]. Strongly positive J amplifies the attraction among units with similar phases, inducing two dynamic patterns: For weakly negative K, swarmalators form stripelike phase clusters [*active clustering*, Fig. 1(b_1)]; for strongly negative K, units with similar phases align into lines that move collectively [*active traveling*, Fig. 1(b_2)]. We refer to the latter as *active* patterns, as the swarmalators continue to move in the steady state while preserving the global structure.

Interestingly, two distinct patterns emerge for $K = 0$, where the phase dynamics of the swarmalators is governed solely by their natural frequencies and independent of the phase differences between neighbors (see also the Supplemental Material [48]). If $J > 0$, swarmalators with similar phases congregate, constituting *multiple phase waves* circulating and forming a ringlike shape [Fig. 1(b_5)]. As J decreases and becomes negative, the ringlike phase waves dissolve and the swarmalators tend to flip to the opposite phase of the neighbors yet struggle to find the optimal position, forming a disordered spatial arrangement [*irregular asynchrony*, Fig. 1(b_7)].

IV. PHASE TRANSITION

Most of the boundaries between the seven patterns described above are well captured by the abrupt changes in either of the three order parameters, ξ, n_v, and R (see Fig. S2 in the Supplemental Material [48]). Yet, one intriguing phase transition appears to be an exception. Along the vertical line where $K = 0$ in the phase diagram (Fig. 1), the topological swarmalators undergo a phase transition from *irregular asynchrony* [Fig. 1(b_7)] to circulating phase waves [Fig. 1(b_5)] at $J = 0$, where ξ diverges while neither n_v nor R shows clear sign of abrupt changes. This transition is analogous to a scenario frequently observed in active matter systems [50] where the internal states of units are "quenched." As a prominently interesting part of the phase diagram, in the following we pay special attention to the emergent "phase wave-asynchrony" transition in topological swarmalators.

At $K = 0$, the swarmalators' phases are frozen (constant in time), such that changes in their collective state result exclusively from their motion according to

$$\dot{\boldsymbol{x}}_i = \sum_{\langle ij \rangle} \frac{\boldsymbol{x}_{ji}}{\|\boldsymbol{x}_{ji}\|}(1 + J\cos(\theta_j - \theta_i)) - \frac{\boldsymbol{x}_{ji}}{\|\boldsymbol{x}_{ji}\|^2}. \tag{5}$$

In their equilibrium locations, we approximate the discrete phase values of the swarmalators by a continuous phase field and interpret resulting vortices as particles in analogy with a 2D Coulomb gas such that a subsequent renormalization group analysis (see Refs. [51–53] and in particular the Supplemental Material [48]) yields

$$\xi \sim e^{c_1|J-J^*|^{-\frac{1}{2}}} \tag{6}$$

on both sides of the sole fixed point J^* in phase space, i.e., for $J \to J^*$ both from below and from above, where c_1 is a constant coefficient. Numerically simulating the system (5) confirms that the correlation length ξ indeed decays toward zero on both sides of the fixed point as Eq. (6) indicates [see Figs. 3(a) and 3(b)]. The excellent agreement between the simulation data and the exponential fits in Fig. 3 provides strong evidence for the self-consistency of the theoretical framework developed [48].

Following the thread of the analogy, the high resemblance between the Hamiltonian of the 2D Coulomb gas in a square lattice and that of our system suggests that a similar first-order transition is present here as in the 2D Coulomb gas system [48]. In addition, the presence of a first-order transition is further substantiated by numerical simulations. Both order parameters R, quantifying local phase synchrony, and n_v, the total number of vortices, exhibit clear hysteresis and state coexistence as J is gradually increased or decreased [see Figs. 3(c) and 3(d)].

How do vortices evolve? And how does this evolution depend on the strength J of the impact of phase differences on swarmalator location? In a given system of swarmalators, vortex numbers may increase or decrease by two different

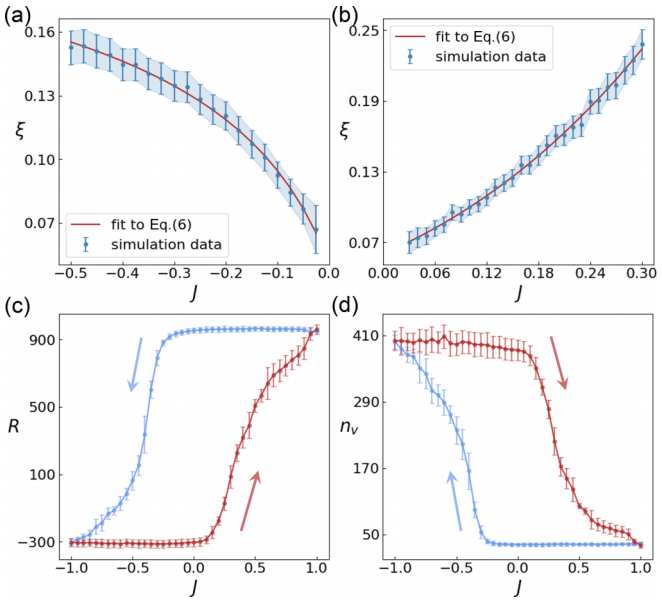

FIG. 3. Discontinuous phase transition: correlation length decay and hysteresis. Order parameters as estimated (points with error bars) from numerical simulations of a system of $N = 1000$ swarmalators, averaged over five realization with randomly varying initial conditions (error bars show standard deviation as a guide). Correlation length for both (a) $J < 0$ and (b) $J > 0$ decays according to the analytical estimates (6), red lines indicate best fits. Both order parameters, (c) phase coherence R and (d) vortex number n_v, indicate hysteresis near $J = 0$, where red and blue lines represent increasing and decreasing J within a single run, respectively. Different system sizes do not alter the correlation length decay and hysteresis (Figs. S5 and S6 in the Supplemental Material [48]). The simulation parameters are listed in Table S1 of the Supplemental Material [48].

processes [Fig. 4(a)]. First, vortices may leave or enter the system at the boundary of the collection of swarmalators, changing the total vortex number n_v one by one. Second, vortex-antivortex pairs may annihilate or emerge in the bulk of the system, changing n_v by integer multiples of 2. Thus, the total winding number $q = n_+ - n_-$, where n_+ and n_- denote the number of vortices and antivortices, respectively, is *not topological invariant*, an important distinction from common models of statistical physics such as the XY model [54] and rather similar to processes in biological systems such as pinwheel annihilation in the visual cortex [55] and other active systems [56]. From random initial conditions, our swarmalator systems tend to generate more vortices if $J < 0$ and suppress them if $J > 0$ [Figs. 4(b)–4(d)]. Moreover, for $J > 0$, we observe that remaining vortices evolve into spatial holes (without swarmalators) over time, suggesting that vortices have a tangible spatial manifestation beyond being mere features of the dynamical or phase fields.

V. CONCLUSIONS

Inspired by recent observations across various active systems, we have introduced a topological swarmalator model where units are coupled topologically on a Delaunay network. Such network-based interactions yield patterns with local vortices indicating phase defects as well as several collective

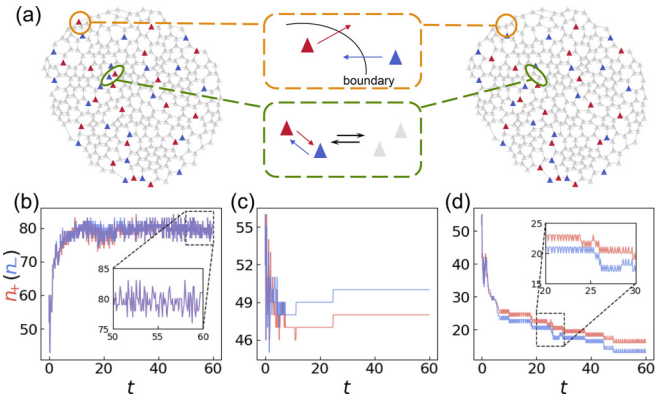

FIG. 4. Dynamics of vortices. (a) Number of vortices changes by two mechanisms: the generation or disappearance of vortices as they enter or leave the system boundary (orange box) and the creation or annihilation of vortex-antivortex pairs in the system's bulk (green box). (b)–(d) Evolution of the vortex numbers in a topological swarmalator system with $N = 200$ units. (b) For $J < 0$, both vortex and antivortex numbers grow and saturate at large values, exhibiting stochastic fluctuations in steady state. (c) For $J = 0$, the vortex numbers stabilize to intermediate-size constants. (d) For $J > 0$, the vortex numbers decay with time. Red and blue lines indicate the number n_+ of vortices and the number n_- of antivortices, respectively.

patterns not observed before. These phenomena are qualitatively different from those observed in models with purely distance-based coupling [46,47]. Although the model class of topological swarmalators introduced here does not describe the details of biological or physical active matter systems, the observed patterns qualitatively resemble those seen in active matter experiments [42,43,45], suggesting a potentially shared underlying mechanism.

We have mapped the phase diagram with three order parameters and analytically identified a first-order phase transition in a regime with active motion but static phase relations, orthogonal to the celebrated Kuramoto model, constituting a core piece of jigsaw puzzle in the whole picture of the physics of topologically interacting active swarmalators and other agents. Furthermore, the theoretical framework developed and employed in this work abandoned conventional Ott-Antonsen ansatz and its variants (2D) as well as the self-consistency equations (1D ring) and instead has extended renormalization group analysis from static lattices to systems with dynamic, state-dependent couplings. These advances may open avenues for the analytical study of a broader class of active matter systems.

ACKNOWLEDGMENTS

This project was funded by the National Natural Science Foundation of China (Grants No. 12375036, No. T2225022, and No. 12350710786), and partially supported by a grant of the German Science Foundation (DFG, Grant No. TI 629/13-1, Project No. 534825001) to M.T.

DATA AVAILABILITY

The data that support the findings of this article are openly available [62].

[1] J. Toner, Y. Tu, and S. Ramaswamy, Hydrodynamics and phases of flocks, Ann. Phys. **318**, 170 (2005).

[2] T. Vicsek and A. Zafeiris, Collective motion, Phys. Rep. **517**, 71 (2012).

[3] S. H. Strogatz, From Kuramoto to Crawford: Exploring the onset of synchronization in populations of coupled oscillators, Physica D **143**, 1 (2000).

[4] J. A. Acebrón, L. L. Bonilla, C. J. Pérez Vicente, F. Ritort, and R. Spigler, The Kuramoto model: A simple paradigm for synchronization phenomena, Rev. Mod. Phys. **77**, 137 (2005).

[5] S. Strogatz, S. Walker, J. M. Yeomans, C. Tarnita, E. Arcaute, M. De Domenico, O. Artime, and K.-I. Goh, Fifty years of 'more is different', Nat. Rev. Phys. **4**, 508 (2022).

[6] G. M. Whitesides and B. Grzybowski, Self-assembly at all scales, Science **295**, 2418 (2002).

[7] O. Feinerman, I. Pinkoviezky, A. Gelblum, E. Fonio, and N. S. Gov, The physics of cooperative transport in groups of ants, Nat. Phys. **14**, 683 (2018).

[8] Y. Kuramoto, Self-entrainment of a population of coupled nonlinear oscillators, in *International Symposium on Mathematical Problems in Theoretical Physics: January 23–29, 1975, Kyoto University, Kyoto, Japan*, edited by H. Araki (Springer, New York, 1975), pp. 420–422.

[9] T. Vicsek, A. Czirók, E. Ben-Jacob, I. Cohen, and O. Shochet, Novel type of phase transition in a system of self-driven particles, Phys. Rev. Lett. **75**, 1226 (1995).

[10] D. Tanaka, General chemotactic model of oscillators, Phys. Rev. Lett. **99**, 134103 (2007).

[11] M. Iwasa and D. Tanaka, Dimensionality of clusters in a swarm oscillator model, Phys. Rev. E **81**, 066214 (2010).

[12] K. P. O'Keeffe, H. Hong, and S. H. Strogatz, Oscillators that sync and swarm, Nat. Commun. **8**, 1504 (2017).

[13] Z. T. Liu, Y. Shi, Y. Zhao, H. Chaté, X.-Q. Shi, and T. H. Zhang, Activity waves and freestanding vortices in populations of subcritical quincke rollers, Proc. Natl. Acad. Sci. USA **118**, e2104724118 (2021).

[14] B. Liebchen and D. Levis, Collective behavior of chiral active matter: Pattern formation and enhanced flocking, Phys. Rev. Lett. **119**, 058002 (2017).

[15] B. Zhang, A. Sokolov, and A. Snezhko, Reconfigurable emergent patterns in active chiral fluids, Nat. Commun. **11**, 4401 (2020).

[16] B. Ventejou, H. Chaté, R. Montagne, and X.-Q. Shi, Susceptibility of orientationally ordered active matter to chirality disorder, Phys. Rev. Lett. **127**, 238001 (2021).

[17] U. Schilcher, C. W. Rauter, and C. Bettstetter, Radii of emergent patterns in swarmalator systems, in *2023 IEEE International Conference on Autonomic Computing and Self-Organizing Systems (ACSOS)* (IEEE, Toronto, ON, Canada, 2023), pp. 151–156.

[18] A. Barciś, M. Barciś, and C. Bettstetter, Robots that sync and swarm: A proof of concept in ROS 2, in *2019 International Symposium on Multi-Robot and Multi-Agent Systems (MRS)* (IEEE, New Brunswick, NJ, 2019), pp. 98–104.

[19] S. Ceron, G. Gardi, K. Petersen, and M. Sitti, Programmable self-organization of heterogeneous microrobot collectives, Proc. Natl. Acad. Sci. USA **120**, e2221913120 (2023).

[20] C. Tomaselli, D. C. Guastella, G. Muscato, L. Minati, M. Frasca, and L. V. Gambuzza, Synchronization of moving chaotic robots, IEEE Rob. Autom. Lett. **9**, 6496 (2024).

[21] Y. Wang, H. Chen, L. Xie, J. Liu, L. Zhang, and J. Yu, Swarm autonomy: From agent functionalization to machine intelligence, Adv. Mater. **37**, 2312956 (2025).

[22] K. P. O'Keeffe and H. Hong, Swarmalators on a ring with distributed couplings, Phys. Rev. E **105**, 064208 (2022).

[23] H. Hong, K. P. O'Keeffe, J. S. Lee, and H. Park, Swarmalators with thermal noise, Phys. Rev. Res. **5**, 023105 (2023).

[24] S. Yoon, K. P. O'Keeffe, J. Mendes, and A. Goltsev, Sync and swarm: Solvable model of nonidentical swarmalators, Phys. Rev. Lett. **129**, 208002 (2022).

[25] J. U. Lizárraga and M. A. de Aguiar, Synchronization of Sakaguchi swarmalators, Phys. Rev. E **108**, 024212 (2023).

[26] G. K. Sar, M. S. Anwar, M. Moriamé, D. Ghosh, and T. Carletti, Strategy to control synchronized dynamics in swarmalator systems, Phys. Rev. E **111**, 034212 (2025).

[27] Z. Cai, Z. Liu, S. Guan, J. Kurths, and Y. Zou, High-mode coupling yields multicoherent-phase phenomena in nonlocally coupled oscillators, Phys. Rev. Lett. **133**, 227201 (2024).

[28] Y. Lu, Y. Xu, W. Cai, Z. Tian, J. Xu, S. Wang, T. Zhu, Y. Liu, M. Wang, Y. Zhou, C. Yan, C. Li, and Z. Zheng, Self-organized circling, clustering and swarming in populations of chiral swarmalators, Chaos Soliton. Fract. **191**, 115794 (2025).

[29] F. Jiménez-Morales, Oscillatory behavior in a system of swarmalators with a short-range repulsive interaction, Phys. Rev. E **101**, 062202 (2020).

[30] J. U. Lizarraga and M. A. de Aguiar, Synchronization and spatial patterns in forced swarmalators, Chaos **30**, 053112 (2020).

[31] S. Ceron, W. Xiao, and D. Rus, Reciprocal and non-reciprocal swarmalators with programmable locomotion and formations for robot swarms, in *2024 IEEE International Conference on Robotics and Automation (ICRA)* (IEEE, Yokohama, Japan, 2024), pp. 12233–12239.

[32] G. K. Sar, S. N. Chowdhury, M. Perc, and D. Ghosh, Swarmalators under competitive time-varying phase interactions, New J. Phys. **24**, 043004 (2022).

[33] N. Blum, A. Li, K. P. O'Keeffe, and O. Kogan, Swarmalators with delayed interactions, Phys. Rev. E **109**, 014205 (2024).

[34] H. Hong, K. Yeo, and H. K. Lee, Coupling disorder in a population of swarmalators, Phys. Rev. E **104**, 044214 (2021).

[35] A. Yadav, V. Chandrasekar, W. Zou, J. Kurths, and D. Senthilkumar, Exotic swarming dynamics of high-dimensional swarmalators, Phys. Rev. E **109**, 044212 (2024).

[36] S. Ceron, K. P. O'Keeffe, and K. Petersen, Diverse behaviors in non-uniform chiral and non-chiral swarmalators, Nat. Commun. **14**, 940 (2023).

[37] S. J. Kongni, V. Nguefoue, T. Njougouo, P. Louodop, F. F. Ferreira, R. Tchitnga, and H. A. Cerdeira, Phase transitions on a multiplex of swarmalators, Phys. Rev. E **108**, 034303 (2023).

[38] S. Ghosh, G. K. Sar, S. Majhi, and D. Ghosh, Antiphase synchronization in a population of swarmalators, Phys. Rev. E **108**, 034217 (2023).

[39] M. Ballerini, N. Cabibbo, R. Candelier, A. Cavagna, E. Cisbani, I. Giardina, V. Lecomte, A. Orlandi, G. Parisi, A. Procaccini, M. Viale, and V. Zdravkovic, Interaction ruling animal collective behavior depends on topological rather than metric distance: Evidence from a field study, Proc. Natl. Acad. Sci. USA **105**, 1232 (2008)

[40] I. H. Riedel, K. Kruse, and J. Howard, A self-organized vortex array of hydrodynamically entrained sperm cells, Science **309**, 300 (2005).

[41] A. P. Petroff, X.-L. Wu, and A. Libchaber, Fast-moving bacteria self-organize into active two-dimensional crystals of rotating cells, Phys. Rev. Lett. **114**, 158102 (2015).

[42] A. Be'er, B. Ilkanaiv, R. Gross, D. B. Kearns, S. Heidenreich, M. Bär, and G. Ariel, A phase diagram for bacterial swarming, Commun. Phys. **3**, 66 (2020).

[43] D. Ghosh and X. Cheng, To cross or not to cross: Collective swimming of *Escherichia coli* under two-dimensional confinement, Phys. Rev. Res. **4**, 023105 (2022).

[44] M. Riedl, I. Mayer, J. Merrin, M. Sixt, and B. Hof, Synchronization in collectively moving inanimate and living active matter, Nat. Commun. **14**, 5633 (2023).

[45] H. Xu and Y. Wu, Self-enhanced mobility enables vortex pattern formation in living matter, Nature (London) **627**, 553 (2024).

[46] F. Ginelli and H. Chaté, Relevance of metric-free interactions in flocking phenomena, Phys. Rev. Lett. **105**, 168103 (2010).

[47] H. K. Lee, K. Yeo, and H. Hong, Collective steady-state patterns of swarmalators with finite-cutoff interaction distance, Chaos **31**, 033134 (2021).

[48] See Supplemental Material at http://link.aps.org/supplemental/10.1103/kghb-vpst for more details of the theoretical framework and the methods, which includes Ref. [57–61]. Supplemental videos demonstrate the seven typical collective dynamics and the emergence of the corresponding patterns.

[49] M. Schröder, M. Timme, and D. Witthaut, A universal order parameter for synchrony in networks of limit cycle oscillators, Chaos **27**, 073119 (2017).

[50] W. Wang, J. Giltinan, S. Zakharchenko, and M. Sitti, Dynamic and programmable self-assembly of micro-rafts at the air-water interface, Sci. Adv. **3**, e1602522 (2017).

[51] J. M. Kosterlitz and D. J. Thouless, Ordering, metastability and phase transitions in two-dimensional systems, J. Phys. C **6**, 1181 (1973).

[52] B. Nienhuis, Coulomb gas formulation of two-dimensional phase transitions, in *Phase Transitions and Critical Phenomena* (Academic Press, London, 1987), Vol. 11, pp. 1–53.

[53] I. Nándori, U. D. Jentschura, K. Sailer, and G. Soff, Renormalization-group analysis of the generalized sine-Gordon model and of the Coulomb gas for $d > \sim 3$ dimensions, Phys. Rev. D **69**, 025004 (2004).

[54] B. G. Bravo, B. D. J. Hernández, and W. Bietenholz, Semi-vortices and cluster-vorticity: New concepts in the Berezinskii-Kosterlitz-Thouless phase transition, Supl. Rev. Mex. Fis. **3**, 020724 (2022).

[55] F. Wolf and T. Geisel, Spontaneous pinwheel annihilation during visual development, Nature (London) **395**, 73 (1998).

[56] A. Doostmohammadi, J. Ignés-Mullol, J. M. Yeomans, and F. Sagués, Active nematics, Nat. Commun. **9**, 3246 (2018).

[57] S. H. Strogatz, *Nonlinear Dynamics and Chaos: With Applications to Physics, Biology, Chemistry, and Engineering* (CRC Press, Boca Raton, FL, 2018).

[58] P. Minnhagen, The two-dimensional Coulomb gas, vortex unbinding, and superfluid-superconducting films, Rev. Mod. Phys. **59**, 1001 (1987).

[59] J. M. Kosterlitz, The critical properties of the two-dimensional *XY* model, J. Phys. C **7**, 1046 (1974).

[60] J.-R. Lee and S. Teitel, New critical behavior in the dense two-dimensional classical Coulomb gas, Phys. Rev. Lett. **64**, 1483 (1990).

[61] J.-R. Lee and S. Teitel, Phase transitions in classical two-dimensional lattice Coulomb gases, Phys. Rev. B **46**, 3247 (1992).

[62] https://github.com/GouGou-root/Topological-Swarmalator.git.